Springer

Journal of Mechanical Science and Technology 23 (2009) 81~88

Journal of
Mechanical
Science and
Technology

www.springerlink.com/content/1738-494x
DOI 10.1007/s12206-008-0926-3

The application of the pseudospectral method to the analysis of helical springs of arbitrary shape †

Jinhee Lee*

Department of Mechano-Informatics, Hongik University, Choongnam 339-701, Korea

(Manuscript Received April 24, 2008; Revised September 20, 2008; Accepted September 23, 2008)

Abstract

The pseudospectral method is applied to the static analysis of helical springs of arbitrary shape. The displacements and the rotations are approximated by series expansions of Chebyshev polynomials. The entire domain is considered as a single element and the governing equations are collocated to yield the system of algebraic equations. The boundary conditions are considered as the constraints, and the set of equations is condensed so that the number of degrees of freedom of the problem matches the total number of the expansion coefficients. Displacements and rotations are computed for noncylindrical helical springs as well as cylindrical helical springs, and parameters that affect the convergence of the solution are discussed.

Keywords: Helical springs; Noncylindrical shape; Pseudospectral method; Chebyshev polynomials

1. Introduction

Helical springs are essential elements of mechanical systems, and their mechanical behaviors are extensively investigated. The finite element method is one of the most popular approaches in the analysis of helical springs. Cook computed the deflection and the stress of a helical spring by the finite element method where there was a single displacement degree of freedom for each node [1]. Omurtag and Aköz introduced a two-node finite element with 2×12 degrees of freedom for helical beams based on a mixed formulation where the shear effects had been taken into consideration [2]. Jiang and Henshall developed a finite element model for helical springs where only a slice of the wire cross section was modeled [3]. Choi and Lim formulated two-node and three-node general curved beam elements on the basis of assumed strain fields on Timoshenko's beam theory [4]. Taktak *et al.* [5] and Fakhreddine *et al.* [6] introduced two-node helical spring elements based on the mixed-hybrid formulations.

Various analytical and semi-analytical methods have also been proposed to assist the analysis of the helical springs. Nagaya derived analytical solutions based on the three-dimensional curved beam theory, and obtained stress expressions by means of Fourier expansion collocation method [7]. Kamiya and Kita applied the boundary element method of quasi-harmonic differential equation to solve the stress distribution of a helical spring and to search for the design synthesis of the optimal shape [8]. Haktanir and Kiral [9] and Haktanir [10] employed stiffness matrix methods to study the helicoidal structures.

The pseudospectral method can be considered as a spectral method that performs a collocation process. Various functions can be selected as the basis functions of the pseudospectral method. Fourier series are suitable for problems with periodic boundary conditions. Chebyshev polynomials are selected for most non-periodic problems. Legendre polynomials are the alternative choices for Chebyshev polynomials and

† This paper was recommended for publication in revised form by Associate Editor Jeong Sam Han

* Corresponding author. Tel.: +82 41 860 2589, Fax.: +82 41 862 2664
E-mail address: jinhlee@hongik.ac.kr

also are the latitudinal factor for the axisymmetric spherical harmonics for the problems in spherical geometry. Gegenbauer polynomials are useful when they are employed as the latitudinal factors for the spherical harmonics. Hermite functions are applied for the problems with doubly infinite intervals. Since each spectral coefficient is determined by all the collocation point values, the pseudospectral method can be made as spatially accurate as desired through exponential rate of convergence with collocation point refinement [11].

Lee applied the pseudospectral method to compute the natural frequencies and the mode shapes of cylindrical and noncylindrical helical springs [12, 13]. In present study, the pseudospectral method using Chebyshev polynomials as the basis functions is applied to the static analysis of helical springs of arbitrary shape.

2. Formulations for helical springs

Figs. 1 and. 2 describe the different types of helical springs and the schematic geometry of a helical spring. The horizontal radius R is constant for cylindrical helical springs and is given for barrel and hyperboloidal types from

$$R(\theta) = R_1 + (R_2 - R_1)\left(1 - \frac{2\theta}{\Theta}\right)^2 \tag{1}$$

where $(0 \le \theta \le \Theta = 2\pi n_c)$ and n_c is the number of turns of the helix.

Assuming the centroid of the cross-section and the shear centerline to coincide and neglecting the warping of the cross-section due to torsion, the static equilibrium equations of a helical spring are derived as follows [7]:

$$F_t' - C\,F_n = 0\,, \quad F_n' + C\,F_t - S\,F_b = 0\,, \tag{2a,b}$$

$$F_b' + S\,F_n = 0\,, \quad M_t' - C\,M_n = 0\,, \tag{2c,d}$$

$$M_n' - \frac{R}{C}F_b + CM_t - SM_b = 0\,,\ M_b' + \frac{R}{C}F_n + SM_n = 0 \tag{2e,f}$$

where the notation ' stands for the differentiation with respect to θ. F_t, F_n and F_b are the components of the internal forces, and M_t, M_n and M_b are the components of the internal moments shown in Fig. 3. Subscripts t, n and b stand for the tangential direction, the normal direction and the binormal direction, respectively. C and S represent $\cos\alpha$ and $\sin\alpha$, where α is the pitch angle of the helix.

The components of internal forces and moments are defined as [7]:

$$F_t = EAC\frac{U_t'}{R} - EAC^2\frac{U_n}{R}, \tag{3a}$$

$$F_n = \frac{GAC}{k}\frac{U_n'}{R} + \frac{GAC^2}{k}\frac{U_t}{R} - \frac{GACS}{k}\frac{U_b}{R} - \frac{GA}{k}\Omega_b, \tag{3b}$$

$$F_b = \frac{GAC}{k}\frac{U_b'}{R} + \frac{GACS}{k}\frac{U_n}{R} + \frac{GA}{k}\Omega_n\,, \tag{3c}$$

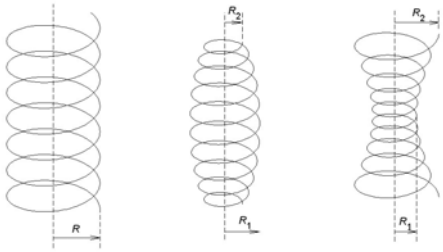

(a) Cylindrical (b) Barrel (c) Hyperbotoidal

Fig. 1. Different types of helical springs.

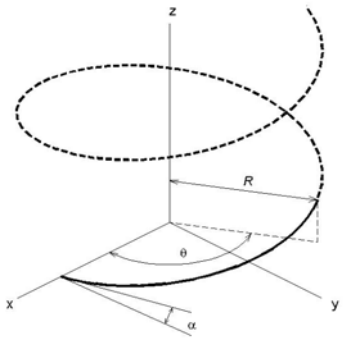

Fig. 2. Schematic geometry of a helical spring.

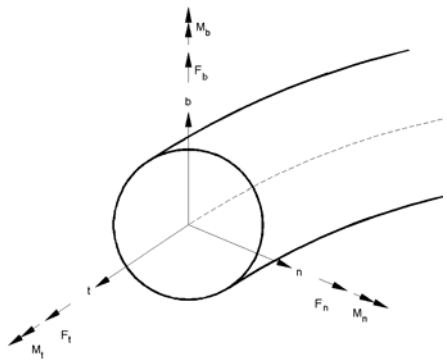

Fig. 3. Components of internal forces and internal moments.

$$M_t = GJC\frac{\Omega_t'}{R} - GJC^2\frac{\Omega_n}{R}, \tag{3d}$$

$$M_n = EI_nC\frac{\Omega_n'}{R} + EI_nC^2\frac{\Omega_t}{R} - EI_nCS\frac{\Omega_b}{R}, \tag{3e}$$

$$M_b = EI_bC\frac{\Omega_b'}{R} + EI_bCS\frac{\Omega_n}{R}. \tag{3f}$$

U_t, U_n and U_b represent the displacements, and Ω_t, Ω_n and Ω_b are the rotations. E, G and k are Young's modulus, the shear modulus and Timoshenko coefficient, respectively. A, I_n, I_b and J are the cross sectional area, the second moments of area with respect to the normal axis and to the binormal axis, and the torsional moment of inertia of the cross section.

The substitution of Eqs. (3a)- (3f) into Eqs. (2a)-(2f) yields the following set of governing equations:

$$\frac{EAC}{R}U_t'' - \frac{EAR'C}{R^2}U_t' - \frac{GAC^3}{kR}U_t - \left(EA + \frac{GA}{k}\right)\frac{C^2}{R}U_n' + \frac{EAR'C^2}{R^2}U_n + \frac{GAC^2S}{kR}U_b + \frac{GAC}{k}\Omega_b = 0, \tag{4a}$$

$$\left(EA + \frac{GA}{k}\right)\frac{C^2}{R}U_t' - \frac{GAR'C^2}{kR^2}U_t + \frac{GAC}{kR}U_n'' - \frac{GAR'C}{kR^2}U_n' - \left(EAC^2 + \frac{GAS^2}{k}\right)\frac{C}{R}U_n - \frac{2GACS}{kR}U_b' + \frac{GAR'CS}{kR^2}U_b - \frac{GAS}{k}\Omega_n - \frac{GA}{k}\Omega_b' = 0, \tag{4b}$$

$$\frac{GAC^2S}{kR}U_t + \frac{2GACS}{kR}U_n' - \frac{GAR'CS}{kR^2}U_n + \frac{GAC}{kR}U_b'' - \frac{GAR'C}{kR^2}U_b' - \frac{GACS^2}{kR}U_b + \frac{GA}{k}\Omega_n' - \frac{GAS}{k}\Omega_b = 0, \tag{4c}$$

$$\frac{GJC}{R}\Omega_t'' - \frac{GJR'C}{R^2}\Omega_t' - \frac{EI_nC^3}{R}\Omega_t - (GJ + EI_n)\frac{C^2}{R}\Omega_n' + \frac{GJR'C^2}{R^2}\Omega_n + \frac{EI_nC^2S}{R}\Omega_b = 0, \tag{4d}$$

$$-\frac{GAS}{k}U_n - \frac{GA}{k}U_b' + (EI_n + GJ)\frac{C^2}{R}\Omega_t' - \frac{EI_nR'C^2}{R^2}\Omega_t + \frac{EI_nC}{R}\Omega_n'' - \frac{EI_nR'C}{R^2}\Omega_n' - \left(\frac{GAR}{kC} + \frac{GJC^3}{R} + \frac{EI_bCS^2}{R}\right)\Omega_n - (EI_n + EI_b)\frac{CS}{R}\Omega_b' + \frac{EI_nR'CS}{R^2}\Omega_b = 0, \tag{4e}$$

$$\frac{GAC}{k}U_t + \frac{GA}{k}U_n' - \frac{GAS}{k}U_b + \frac{EI_nC^2S}{R}\Omega_t + (EI_b + EI_n)\frac{CS}{R}\Omega_n' - \frac{EI_bR'CS}{R^2}\Omega_n + \frac{EI_bC}{R}\Omega_b'' - \frac{EI_bR'C}{R^2}\Omega_b' - \left(\frac{GAR}{kC} + \frac{EI_nCS^2}{R}\right)\Omega_b = 0. \tag{4f}$$

When the range of the independent variable is given by $(0 \le \theta \le \Theta)$, it is convenient to use the normalized variable

$$\xi = \frac{2\theta - \Theta}{\Theta} \in [-1,1]. \tag{5}$$

The displacements and rotations are then expressed as sums of Chebyshev polynomials as follows:

$$\begin{aligned} U_t(\xi) &= \sum_{k=1}^{K+2} a_k T_{k-1}(\xi), \quad U_n(\xi) = \sum_{k=1}^{K+2} b_k T_{k-1}(\xi), \\ U_b(\xi) &= \sum_{k=1}^{K+2} c_k T_{k-1}(\xi), \quad \Omega_t(\xi) = \sum_{k=1}^{K+2} d_k T_{k-1}(\xi), \\ \Omega_n(\xi) &= \sum_{k=1}^{K+2} e_k T_{k-1}(\xi), \quad \Omega_b(\xi) = \sum_{k=1}^{K+2} f_k T_{k-1}(\xi), \end{aligned} \tag{6}$$

where a_k, b_k, c_k, d_k, e_k and f_k are the expansion coefficients. K and T_{k-1} are the number of collocation points and the Chebyshev polynomial of the first kind of degree of $k-1$, respectively. The series expansions of Eq. (6) are substituted into Eqs. (4a)- (4f), and are collocated at the Gauss-Lobatto collocation points

$$\xi_i = -\cos\frac{\pi(2i-1)}{2K} \quad (i = 1,2,\cdots,K) \tag{7}$$

to yield the collocated governing equations given in Appendix. The collocated governing equations (A1)- (A6) can be rearranged in the matrix form

$$[B]\{\delta\} + [D]\{\gamma\} = \{0\} \tag{8}$$

where the vectors in Eq. (8) are defined by

$$\begin{aligned} \{\delta\} = \{&a_1\ a_2 \cdots a_K\ b_1\ b_2 \cdots b_K\ c_1\ c_2 \cdots c_K \\ &d_1\ d_2 \cdots d_K\ e_1\ e_2 \cdots e_K\ f_1 f_2 \cdots f_K\}^T \\ \{\gamma\} = \{&a_{K+1}\ a_{K+2}\ b_{K+1}\ b_{K+2}\ c_{K+1}\ c_{K+2} \\ &d_{K+1}\ d_{K+2}\ e_{K+1}\ e_{K+2}\ f_{K+1}\ f_{K+2}\}^T \end{aligned} \tag{9}$$

and $\{0\}$ is a zero vector. The total number of equations in Eq. (8) is 6*K*, whereas the total number of unknown expansion coefficients in Eq. (6) is 6 (*K*+2). The remaining twelve equations are obtained from the boundary conditions. Typical boundary conditions include

clamped:

$$U_t = 0, U_n = 0, U_b = 0, \Omega_t = 0, \Omega_n = 0, \Omega_b = 0, \quad (10a)$$

hinged:

$$U_t = 0, U_n = 0, U_b = 0, M_t = 0, M_n = 0, M_b = 0, \quad (10b)$$

loaded by axial force F:

$$F_t \cos\alpha - F_b \sin\alpha = 0,\ F_t \sin\alpha + F_b \cos\alpha = F,\ F_n = 0,\ M_t = 0,\ M_n = 0,\ M_b = 0. \quad (10c)$$

Assume, for example, that the helical spring is clamped at one end and an axial force F is applied at the other end, then the boundary condition is expressed as Eq. (10a) at $\xi = -1$ and Eq. (10c) at $\xi = 1$, which are expressed by the series expansions of Eq. (6) to give the following:

$$\begin{aligned}
&\sum_{k=1}^{K+2} a_k T_{k-1}(-1) = 0, \quad \sum_{k=1}^{K+2} b_k T_{k-1}(-1) = 0,\\
&\sum_{k=1}^{K+2} c_k T_{k-1}(-1) = 0, \quad \sum_{k=1}^{K+2} d_k T_{k-1}(-1) = 0,\\
&\sum_{k=1}^{K+2} e_k T_{k-1}(-1) = 0, \quad \sum_{k=1}^{K+2} f_k T_{k-1}(-1) = 0,\\
&\sum_{k=1}^{K+2}\left\{ a_k \frac{2EAC^2}{R\Theta} T^*_{k-1}(1) - b_k\left(\frac{EAC^3}{R} + \frac{GACS^2}{kR}\right) T_{k-1}(1) \right.\\
&\qquad \left. - c_k \frac{2GACS}{kR\Theta} T^*_{k-1}(1) - e_k \frac{GAS}{k} T_{k-1}(1)\right\} = 0,\\
&\sum_{k=1}^{K+2}\left\{ a_k \frac{2EACS}{R\Theta} T^*_{k-1}(1) + b_k \frac{C^2S}{R}\left(-EA + \frac{GA}{k}\right) T_{k-1}(1) \right.\\
&\qquad \left. + c_k \frac{2GAC^2}{kR\Theta} T^*_{k-1}(1) + e_k \frac{GAC}{k} T_{k-1}(1)\right\} = F,\\
&\sum_{k=1}^{K+2}\left\{ a_k \frac{GAC^2}{kR} T_{k-1}(1) + b_k \frac{2GAC}{kR\Theta} T^*_{k-1}(1) \right.\\
&\qquad \left. - c_k \frac{GACS}{kR} T_{k-1}(1) - f_k \frac{GA}{k} T_{k-1}(1)\right\} = 0,\\
&\sum_{k=1}^{K+2}\left\{ d_k \frac{2GJC}{R\Theta} T^*_{k-1}(1) - e_k \frac{GJC^2}{R} T_{k-1}(1)\right\} = 0,\\
&\sum_{k=1}^{K+2}\left\{ d_k \frac{EI_nC^2}{R} T_{k-1}(1) + e_k \frac{2EI_nC}{R\Theta} T^*_{k-1}(1) \right.\\
&\qquad \left. - f_k \frac{EI_nCS}{R} T_{k-1}(1)\right\} = 0,\\
&\sum_{k=1}^{K+2}\left\{ e_k \frac{EI_bCS}{R} T_{k-1}(1) + f_k \frac{2EI_bC}{R\Theta} T^*_{k-1}(1)\right\} = 0.
\end{aligned} \quad (11)$$

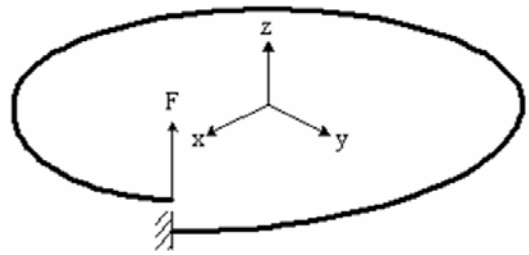

Fig. 4. One coiled helical spring.

The notation $*$ stands for the differentiations with respect to ξ. The boundary condition set (11) can be rearranged in the matrix form:

$$[V]\{\delta\} + [W]\{\gamma\} = \{L\} \quad (12)$$

Since $\{\gamma\}$ in Eq. (12) can be expressed as

$$\{\gamma\} = [W]^{-1}\left(\{L\} - [V]\{\delta\}\right), \quad (13)$$

Eq. (8) can be reformulated as

$$\left([B] - [D][W]^{-1}[V]\right)\{\delta\} = -[D][W]^{-1}\{L\}. \quad (14)$$

Eq. (14) is solved for the estimates for the expansion coefficients. Once the expansion coefficients are obtained, the components of internal forces and internal moments are computed by

$$F_t = \frac{2EAC}{R\Theta}\sum_{k=1}^{K+2} a_k T^*_{k-1}(\xi) - \frac{EAC^2}{R}\sum_{k=1}^{K+2} b_k T_{k-1}(\xi), \quad (15a)$$

$$F_n = \frac{2GAC}{kR\Theta}\sum_{k=1}^{K+2} b_k T^*_{k-1}(\xi) + \frac{GAC^2}{kR}\sum_{k=1}^{K+2} a_k T_{k-1}(\xi) - \frac{GACS}{kR}\sum_{k=1}^{K+2} c_k T_{k-1}(\xi) - \frac{GA}{k}\sum_{k=1}^{K+2} f_k T_{k-1}(\xi), \quad (15b)$$

$$F_b = \frac{2GAC}{kR\Theta}\sum_{k=1}^{K+2} c_k T^*_{k-1}(\xi) + \frac{GACS}{kR}\sum_{k=1}^{K+2} b_k T_{k-1}(\xi) + \frac{GA}{k}\sum_{k=1}^{K+2} e_k T_{k-1}(\xi), \quad (15c)$$

$$M_t = \frac{2GJC}{R\Theta}\sum_{k=1}^{K+2} d_k T^*_{k-1}(\xi) - \frac{GJC^2}{R}\sum_{k=1}^{K+2} e_k T_{k-1}(\xi), \quad (15d)$$

$$M_n = \frac{2EI_nC}{R\Theta}\sum_{k=1}^{K+2} e_k T^*_{k-1}(\xi) + \frac{EI_nC^2}{R}\sum_{k=1}^{K+2} d_k T^*_{k-1}(\xi) - \frac{EI_nCS}{R}\sum_{k=1}^{K+2} f_k T_{k-1}(\xi), \quad (15e)$$

$$M_b = \frac{2EI_bC}{R\Theta}\sum_{k=1}^{K+2} f_k T^*_{k-1}(\xi) + \frac{EI_bCS}{R}\sum_{k=1}^{K+2} e_k T_{k-1}(\xi). \quad (15f)$$

Posteriorly, the components of the stresses of the wire can be computed as:

normal stress due to F_t: $\sigma_t = \frac{F_t}{A}$, (16a)

shear stresses due to F_n and F_b:

$$\tau_{tn} = \frac{F_n}{A},\ \tau_{bt} = \frac{F_b}{A}, \quad (16b,c)$$

bending stresses due to M_n and M_b:

$$(\sigma_t)_n = \frac{M_n y_n}{I_n}, (\sigma_t)_b = \frac{M_b y_b}{I_b}, \quad (16d,e)$$

torsional stress due to M_t: $\tau_{nb} = \frac{M_t r}{J}$. (16f)

where y_n and y_b stand for the distances from the neutral axes and r is the distance from the centroid of the cross-section of the wire.

Neither numerical differentiation nor numerical integration is associated with the present method. The differentiations of Chebyshev polynomials with respect to ξ are performed analytically, which enhances the accuracy of the solution of the pseudospectral method.

3. Numerical examples and discussions

As a preliminary test, a convergence check of the present method is carried out for one coiled helical spring shown in Fig. 4, and the result is given in Table 1. The spring has a constant horizontal radius of R=10 mm. Springs are considered to have circular cross sections throughout this study. The diameter of wire, the pitch angle, Young's modulus, Timoshenko coefficient and Poisson ratio are d=1 mm, α=10°, E=10^7 N/mm^2, k=1.1, and ν=0.3. The spring is clamped at one end and is loaded by axial force F=100 N at another end. Table 1 shows the convergence is achieved for four significant digits for less than K=12 and the result is in excellent agreement with that of Fakhreddine *et al.* [6].

In general it is considered that the convergence is slow for the boundary value problems in an arbitrary domain. A comparison of the convergence behaviors between a cylindrical spring and a barrel type spring is made and the result is given in Table 2. The number of collocation points K required for the convergence of the barrel type spring is much the same as that of the cylindrical spring, which reminds us that the computational geometry of a noncylindrical helical spring is one dimensional, as is that of a cylindrical helical spring.

The effects of spring parameters such as n_c, R and α on K that are required for the convergence of the solution are investigated and the results are given in Tables 3-5. Tables 3-5 show that a larger number of K is required for the convergence of the solution as n_c increases, while the influence of R and α is limited.

A simple free body diagram may indicate that the internal moments are $M_t = -FR$, $M_n = 0$ and $M_b = 0$ when the line of action of the applied force coincides with the centerline of the helix as shown in Fig. 5 (a).

When the line of action of the applied force deviates from the centerline of the helix as shown in Fig. 5 (b), which is the case of present study, the computation becomes rather complicated.

Table 1. Convergence test of the deflection of one coiled helical spring at the loaded point (R=10 mm, d=1 mm, α=10°, E=10^7 N/mm^2, k=1.1, ν=0.3, F=100 N, displacement in mm).

Present method					Fakhreddine *et al* [6]
K=6	K=9	K=12	K=15	K=20	
2.953	3.177	3.169	3.169	3.169	3.169

Table 2. Comparison of the deflection of cylindrical and noncylindrical helical springs at the loaded point as K varies (R_1=10 mm, d=1 mm, α=10°, E=10^7 N/mm^2, k=1.1, ν=0.3, n_c =10, clamped at one end and loaded by axial force F=100 N at another, displacement in mm).

K	20	30	40	50	60
R_2/R_1=0.5	11.634	11.375	12.929	13.800	13.800
R_2/R_1=1	18.564	21.273	28.996	31.691	31.690

Table 3. Number of collocation points K required for the convergence of solution to four figures for different number of turns of the helix n_c (cylindrical helical spring, R=10 mm, d=1 mm, α=10°, E=10^7 N/mm^2, k=1.1, ν=0.3, clamped at one end and loaded by axial force F=100 N at another).

n_c	5	10	15	20	25
K	31	49	71	85	107

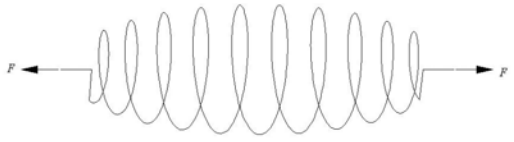

(a) Line of action coincident with the centerline of the helix

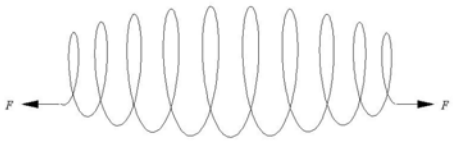

(b) Line of action deviated from the centerline of the helix

Fig. 5. Line of action of the force exerted on the helical spring.

The present method is applied to the analysis of a helical spring of arbitrary shape. The barrel-hyperboloidal type helical spring is clamped at both ends and then the ends are extended by an axial force F=1 N ($U_n = 0$, $\Omega_t = 0$, $\Omega_n = 0$, $\Omega_b = 0$, $F_t \cos\alpha - F_b \sin\alpha = 0$, $F_t \sin\alpha + F_b \cos\alpha = F$ at $\xi = 1$). The ratio R_2/R_1 varies from 0.6 (barrel type) to 1.4 (hyperboloidal type). The horizontal radius at the center, the diameter of wire, the number of turns and the pitch angle are R_1=25mm, d=2mm, n_c=5 and α=10°, respectively. Young's modulus, Poisson's ratio and Timoshenko coefficient are E=210 GPa, ν=0.3 and k=1.1. The computed displacements and rotations are shown in Figs. 6 (a)-(f). The magnitudes of displacements and rotations increase as R_2 increases. It is worthwhile to notice that U_b is the most dominant among the displacement components, while Ω_b is the least dominant among the rotation components. It is also interesting to see that U_n and Ω_n are symmetric about the midpoint, while the others are antisymmetric under given boundary conditions.

Table 4. Number of collocation points K required for the convergence of solution to four figures for different horizontal radius R (cylindrical helical spring, n_c=10, d=1 mm, α=10°, E=10^7 N/mm^2, k=1.1, ν=0.3, clamped at one end and loaded by axial force F=100 N at another).

R	5 mm	10 mm	15 mm	20 mm	25 mm
K	47	49	47	49	48

Table 5. Number of collocation points K required for the convergence of solution to four figures for different pitch angle α (cylindrical helical spring, R= 10 mm, n_c=10, d=1 mm, E=10^7 N/mm^2, k=1.1, ν=0.3, clamped at one end and loaded by axial force F=100 N at another).

α	6°	8°	10°	12°
K	47	49	49	49

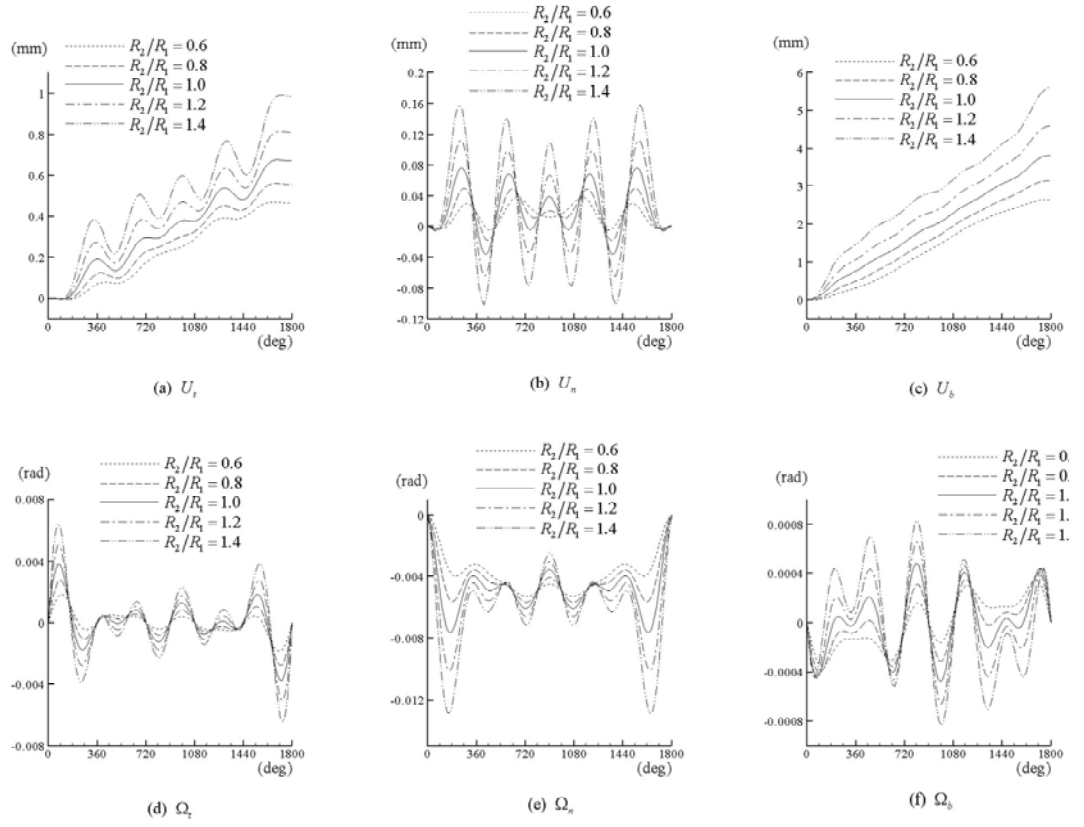

Fig. 6. Displacements and rotations for different R_2/R_1 (circular cross section, R_1=25mm, d=2mm, n_c=5, α=10°, E=210 GPa, ν=0.3, k=1.1, K=60, clamped at both ends and then extended by axial force F=1 N).

4. Conclusions

The pseudospectral method is applied to the analysis of helical springs of arbitrary shape and numerical examples are provided. The displacements and the rotations of the spring are approximated by series expansions of Chebyshev polynomials. The equilibrium equations include $dR/d\theta$ as well as $R(\theta)$ to allow the computations of the noncylindrical helical springs as well as the cylindrical ones, and the entire domain is considered as a single element. The equilibrium equations are collocated at the Gauss-Lobatto points to yield the collocated governing equations, from which the expansion coefficients are computed. To handle the boundary conditions the number of collocation points is chosen to be less than that of the expansion terms. The boundary conditions are considered as the constraints of the governing equations, and the set of algebraic equations is condensed so that the number of degrees of freedom of the problem matches that of the expansion coefficients. Parameters such as the number of turns and the pitch angle that affect the convergence of the solution are discussed.

References

[1] R. D. Cook, Finite element analysis of closely-coiled helical springs, *Computers & Structures*, 34 (1) (1990) 179-180.

[2] M. H. Omurtag and A. Y. Aköz, The mixed finite element solution of helical beams with variable cross-section under arbitrary loading, *Computers & Structures*, 43 (2) (1992) 325-331.

[3] W. G. Jiang and J. L. Henshall, A novel finite element model for helical springs, *Finite Elements in Analysis and Design*, 35 (2000) 363-377.

[4] J.-K. Choi and J.-K. Lim, General curved beam elements based on the assumed strain fields, *Computers & Structures*, 55 (3) (1995) 379-386.

[5] M. Taktak, F. Dammak, S. Abid and M. Haddar, A mixed-hybrid finite element for three-dimensional isotropic helical beam analysis, *International Journal for Mechanical Science*, 47 (2005) 209-229.

[6] D. Fakhreddine, T. Mohamed, S. Abid, D. Abderrazek and H. Mohamed, Finite element method for the stress analysis of isotropic cylindrical helical spring, *European Journal of Mechanics A/Solids*, 24 (2005) 1068-1078.

[7] K. Nagaya, Stress in a helical spring of arbitrary cross section with consideration of end effects, *Journal of Vibration, Acoustics, Stress, and Reliability in Design*, 109 (1987) 289-301.

[8] N. Kamiya and E. Kita, Boundary element method for quasi-harmonic differential equation with application to strss analysis and shape optimization of helical spring, *Computers & Structures*, 37 (1) (1990) 81-86.

[9] V. Haktanir and E. Kiral, Statical analysis of elastically and continuously supported helicoidal structures by the transfer and stiffness matrix method, *Computers & Structures*, 49 (4) (1993) 663-677.

[10] V. Haktanir, The complementary functions method for the element stiffness matrix of arbitrary spatial bars of helicoidal axes, *International Journal for Numerical Methods in Engineering*, 38 (1995) 1031-1056.

[11] J. P. Boyd, *Chebyshev & Fourier Spectral Methods, Lecture Notes in Engineering*, Springer-Verlag, (1989) 20-78.

[12] J. Lee, Free vibration analysis of cylindrical helical springs by the pseudospectral method, *Journal of Sound and Vibration*, 302 (2007) 185-196.

[13] J. Lee, Free vibration analysis of non-cylindrical helical springs by the pseudospectral method, *Journal of Sound and Vibration*, 305 (2007) 543-551.

Appendix

The collocated governing equations are

$$\begin{aligned}
&\sum_{k=1}^{K+2} a_k \left\{ \frac{4EAC}{R_i\Theta^2} T_{k-1}^{**}(\xi_i) - \frac{2EAR_i'C}{R_i^2\Theta} T_{k-1}^{*}(\xi_i) \right. \\
&\qquad \left. - \frac{GAC^3}{kR_i} T_{k-1}(\xi_i) \right\} \\
&+ \sum_{k=1}^{K+2} b_k \left\{ -\left(EA + \frac{GA}{k} \right) \frac{2C^2}{R_i\Theta} T_{k-1}^{*}(\xi_i) + \frac{EAR_i'C^2}{R_i^2} T_{k-1}(\xi_i) \right\} \\
&+ \sum_{k=1}^{K+2} c_k \frac{GAC^2S}{k} T_{k-1}(\xi_i) + \sum_{k=1}^{K+2} f_k \frac{GAC}{k} T_{k-1}(\xi_i) = 0,
\end{aligned} \tag{A.1}$$

$$\begin{aligned}
&\sum_{k=1}^{K+2} a_k \left\{ \left(EA + \frac{GA}{k} \right) \frac{2C^2}{R_i\Theta} T_{k-1}^{*}(\xi_i) - \frac{GAR_i'C^2}{kR_i^2} T_{k-1}(\xi_i) \right\} \\
&+ \sum_{k=1}^{K+2} b_k \left\{ \frac{4GAC}{kR_i\Theta^2} T_{k-1}^{**}(\xi_i) - \frac{2GAR_i'C}{kR_i^2\Theta} T_{k-1}^{*}(\xi_i) \right. \\
&\qquad \left. - -\left(EAC^2 + \frac{GAS^2}{k} \right) \frac{C}{R_i} T_{k-1}(\xi_i) \right\} \\
&+ \sum_{k=1}^{K+2} c_k \left\{ -\frac{4GACS}{kR_i\Theta} T_{k-1}^{*}(\xi_i) + \frac{GAR_i'CS}{kR_i^2} T_{k-1}(\xi_i) \right\} \\
&- \sum_{k=1}^{K+2} e_k \frac{GAS}{k} T_{k-1}(\xi_i) - \sum_{k=1}^{K+2} f_k \frac{2GA}{k\Theta} T_{k-1}^{*}(\xi_i) = 0,
\end{aligned} \tag{A.2}$$

$$\sum_{k=1}^{K+2} a_k \frac{GAC^2S}{kR_i} T_{k-1}(\xi_i)$$
$$+\sum_{k=1}^{K+2} b_k \left\{ \frac{4GACS}{kR_i\Theta} T^*_{k-1}(\xi_i) - \frac{GAR_i'CS}{kR_i^2} T_{k-1}(\xi_i) \right\}$$
$$+\sum_{k=1}^{K+2} c_k \left\{ \frac{4GAC}{kR_i\Theta^2} T^{**}_{k-1}(\xi_i) - \frac{2GAR_i'C}{kR_i^2\Theta} T^*_{k-1}(\xi_i) - \frac{GACS^2}{kR_i} T_{k-1}(\xi_i) \right\} \quad \text{(A.3)}$$
$$+\sum_{k=1}^{K+2} e_k \frac{2GA}{k\Theta} T^*_{k-1}(\xi_i) - \sum_{k=1}^{K+2} f_k \frac{GAS}{k} T_{k-1}(\xi_i) = 0,$$

$$\sum_{k=1}^{K+2} d_k \left\{ \frac{4GJC}{R_i\Theta^2} T^{**}_{k-1}(\xi_i) - \frac{2GJR_i'C}{R_i^2\Theta} T^*_{k-1}(\xi_i) - \frac{EI_nC^3}{R_i} T_{k-1}(\xi_i) \right\}$$
$$+\sum_{k=1}^{K+2} e_k \left\{ -(GJ+EI_n)\frac{2C^2}{R_i\Theta} T^*_{k-1}(\xi_i) + \frac{GJR_i'C^2}{R_i^2} T_{k-1}(\xi_i) \right\} \quad \text{(A.4)}$$
$$+\sum_{k=1}^{K+2} f_k \frac{EI_nC^2S}{R_i} T_{k-1}(\xi_i) = 0,$$

$$-\sum_{k=1}^{K+2} b_k \frac{GAS}{k} T_{k-1}(\xi_i) - \sum_{k=1}^{K+2} c_k \frac{2GA}{k\Theta} T^*_{k-1}(\xi_i)$$
$$+\sum_{k=1}^{K+2} d_k \left\{ (EI_n + GJ)\frac{2C^2}{R_i\Theta} T^*_{k-1}(\xi_i) - \frac{EI_nR_i'C^2}{R_i^2} T_{k-1}(\xi_i) \right\}$$
$$+\sum_{k=1}^{K+2} e_k \left\{ \frac{4EI_nC}{R_i\Theta^2} T^{**}_{k-1}(\xi_i) - \frac{2EI_nR_i'C}{R_i^2\Theta} T^*_{k-1}(\xi_i) \right.$$
$$\left. -\left(\frac{GAR_i}{kC} + \frac{GJC^3}{R_i} + \frac{EI_bCS^2}{R_i} \right) T_{k-1}(\xi_i) \right\} \quad \text{(A.5)}$$
$$+\sum_{k=1}^{K+2} f_k \left\{ -(EI_n + EI_b)\frac{2CS}{R_i\Theta} T^*_{k-1}(\xi_i) + \frac{EI_nR_i'CS}{R_i^2} T_{k-1}(\xi_i) \right\} = 0,$$

$$\sum_{k=1}^{K+2} a_k \frac{GAC}{k} T_{k-1}(\xi_i) + \sum_{k=1}^{K+2} b_k \frac{2GA}{k\Theta} T^*_{k-1}(\xi_i)$$
$$-\sum_{k=1}^{K+2} c_k \frac{GAS}{k} T_{k-1}(\xi_i) + \sum_{k=1}^{K+2} d_k \frac{EI_nC^2S}{R_i} T_{k-1}(\xi_i)$$
$$+\sum_{k=1}^{K+2} e_k \left\{ (EI_n + EI_b)\frac{2CS}{R_i\Theta} T^*_{k-1}(\xi_i) - \frac{EI_bR_i'CS}{R_i^2} T_{k-1}(\xi_i) \right\} \quad \text{(A.6)}$$
$$+\sum_{k=1}^{K+2} f_k \left\{ \frac{4EI_bC}{R_i\Theta^2} T^{**}_{k-1}(\xi_i) - \frac{2EI_bR_i'C}{R_i^2\Theta} T^*_{k-1}(\xi_i) - \left(\frac{GAR_i}{kC} + \frac{EI_nCS^2}{R_i} \right) T_{k-1}(\xi_i) \right\} = 0,$$

$(i = 1, \cdots, K)$.

The notation * stands for the differentiations with respect to ξ. R_i represents $R(\xi_i)$.

Jinhee Lee received B. S. and M. S. degrees from Seoul National Uni-versity and KAIST in 1982 and 1984, respectively. He received his Ph.D. degree from University of Michigan in 1992 and joined Dept. of Mechano-Informatics of Hongik University in Choongnam, Korea. His research interests include inverse problems, pseudospectral method, vibration and dynamic systems.